PECTORALIS MUSCLE FORCE AND POWER OUTPUT DURING DIFFERENT MODES OF FLIGHT IN PIGEONS (*COLUMBA LIVIA*)

KENNETH P. DIAL

Division of Biological Sciences, University of Montana, Missoula, MT 59812, USA

and ANDREW A. BIEWENER

Department of Organismal Biology and Anatomy, University of Chicago, 1025 East 57th Street, Chicago, IL 60637, USA

Summary

In vivo measurements of pectoralis muscle force during different modes of free flight (takeoff, level flapping, landing, vertical ascending and near vertical descending flight) were obtained using a strain gauge attached to the dorsal surface of the delto-pectoral crest (DPC) of the humerus in four trained pigeons (*Columbalivia*). In one bird, a rosette strain gauge was attached to the DPC to determine the principal axis of strain produced by tension of the pectoralis. Strain signals recorded during flight were calibrated to force based on *in situ* measurements of tetanic force and on direct tension applied to the muscle's insertion at the DPC. Rosette strain recordings showed that at maximal force the orientation of tensile principal strain was $-15°$ (proximo-anterior) to the perpendicular axis of the DPC (or $+75°$ to the longitudinal axis of the humerus), ranging from $+15$ to $-25°$ to the DPC axis during the downstroke. The consistency of tensile principal strain orientation in the DPC confirms the more general use of single-element strain gauges as being a reliable method for determining *in vivo* pectoralis force generation. Our strain recordings show that the pectoralis begins to develop force as it is being lengthened, during the final one-third of the upstroke, and attains maximum force output while shortening during the first one-third of the downstroke. Force is sustained throughout the entire downstroke, even after the onset of the upstroke for certain flight conditions. Mean peak forces developed by the pectoralis based on measurements from 40 wingbeats for each bird (160 total) were: 24.9 ± 3.1N during takeoff, 19.7 ± 2.0N during level flight (at speeds of about $6–9\,\mathrm{m\,s}^{-1}$ and a wingbeat frequency of 8.6 ± 0.3Hz), 18.7 ± 2.5N during landing, 23.7 ± 2.7N during near-vertical descent, and 26.0 ± 1.8N during vertical ascending flight. These forces are considerably lower than the maximum isometric force (67N, P_0) of the muscle, ranging from 28% (landing) to 39% (vertical ascending) of P_0. Based on estimates of muscle fiber length change determined from high-speed (200frames s^{-1}) light ciné films taken of the animals, we calculate the mass-specific power output of the pigeon pectoralis to be $51\,\mathrm{W\,kg}^{-1}$ during level flight (approximately $8\,\mathrm{m\,s}^{-1}$), and $119\,\mathrm{W\,kg}^{-1}$ during takeoff from the ground. When the birds were harnessed with weighted backpacks (50% and 100% of body weight), the forces generated by the pectoralis did not significantly exceed those observed in unloaded birds executing

vertical ascending flight. These data suggest that the range of force production by the pectoralis under these differing conditions is constrained by the force–velocity properties of the muscle operating at fairly rapid rates of shortening (4.4 fiberlengths s^{-1} during level flight and 6.7 fiberlengths s^{-1} during takeoff).

Introduction

Our understanding of the magnitude of muscular force and mechanical power output during sustained flapping flight in birds has relied primarily on indirect calculations using fixed-wing aerodynamic theory coupled with kinematic data (Brown, 1963; Greenewalt, 1975, Lighthill, 1977; Pennycuick, 1968, 1975, 1989). Metabolic power requirements for flapping flight derived from oxygen consumption measurements have provided valuable data to evaluate some of the predictions of these models. These data have been reported for birds (Bernstein *et al.* 1973; Rothe and Nachtigall, 1987; Torre-Bueno and LaRochelle, 1978; Tucker, 1968) and, more recently, for bumblebees (Ellington *et al.* 1990).

In general, the results of these studies do not show as pronounced a U-shaped power curve relative to flight speed as predicted by aerodynamic models. Until recently, however, empirical measurements of the mechanical power output of birds' flight muscles have not been possible. In a recent study of the European starling (*Sturnus vulgaris*), we reported a method that enables us to measure directly the force developed by the pectoralis of a bird in free flight (Biewener *et al.* 1992). Our approach is to make *in vivo* recordings of the bone strain developed at the pectoralis muscle's insertion on the humerus, the delto-pectoral crest (DPC). Muscle tension is transduced by a strain gauge attached to the dorsal surface of the DPC, which can subsequently be calibrated to *in situ* measurements of muscle force. Both the magnitude and time course of force·development by the pectoralis during the wingbeat cycle can be obtained using this method.

In our previous study, we measured forces for only one speed of level flight while the birds flew in a wind tunnel. Certain features of the wind tunnel's design also introduced some uncertainty concerning the airspeed and flow conditions experienced by the animals in the flight chamber. In the present study, we measure the forces generated by the pectoralis of the pigeon (*Columbalivia*) during various modes of free flight (takeoff, level flapping flight, landing, vertical ascending flight and near-vertical descending flight), as well as during load carrying. These recordings enable us to evaluate the force and power output of this muscle over a much broader range of its function in this species and to compare these results with those obtained previously for European starlings.

Materials and methods

Animals and training procedures

Four pigeons (body mass: 301–314g) were captured from wild populations in Missoula County, Montana, housed in stainless-steel cages (1m wide×1m deep×1.5 m high) and maintained with commercial pigeon feed, vitamins and water *ad libitum*. Each bird was

trained twice each day (30min per bird) for eight weeks to fly down a hallway (47m long, 2.8 m wide, 2.6m high). The birds were conditioned to take off when placed on the floor, to fly level for approximately 20m, and to land on a perch platform ($0.3m^2$) positioned at a height of 1.3m from the floor. The birds were also trained to fly vertically (ascend) from the floor to a 2.5m high perch positioned directly above them, as well as to descend to the floor. To obtain as steep a descending flight path as possible, the birds were released from the hand to fly down to a perch positioned almost directly below. While all birds were able to ascend vertically (90° angle climb), birds were unable to descend at an angle steeper than 80°. Since the birds generally flew with forward velocities of 6–9ms^{-1} during level fight, these sequences should be considered representative of 'slow flight' as described by Brown (1948). In slow flight, the tail remains slightly depressed and abducted, and the bird's body is oriented at a steeper angle (25–45°) to the flight path.

Cinematography

Using a 16mm camera (Lo-Cam, Red Lakes Laboratory) located at the end of the hallway, light ciné films were obtained at 200frames s^{-1} during the five modes of flight to establish wing position in relation to the recordings of pectoralis muscle force. Thus, anterior views were obtained during takeoff, level flight and landing, whereas lateral views were obtained during ascending and descending flight. An electrical impulse synchronized to each frame of film (Kodak 7250 Ektachrome) was recorded, together with pectoralis electromyogram (EMG) and DPC strain. Twelve 1000-W quartz lights (Tota-Light, T1-10, Lowel Co.) illuminated the flyway. Film was viewed using an L-W (model 224-S) film analyzer, and kinematic measurements were made using a ruler and protractor set against a projection screen. Flight velocity, body angle and flight trajectory were determined from films of level flight taken in lateral view. Anterior film views were used to quantify wing excursion. Humeral excursions were determined by measuring the leading edge of the proximal third of the wing during each 5ms interval (time between successive frames) within a wingbeat cycle. Because humeral position cannot be measured directly from light films, our estimates of muscle length change based on angular displacement of the proximal portion of the wing should be treated with some caution.

Strain gauge and muscle electrode implantation procedures

Birds were anesthetized (25mgkg^{-1} of ketamine and 2mgkg^{-1} of xylazine, supplemented as needed) and the feathers removed over the left shoulder, on the back between the scapulae, and along the ventral aspect of the pectoralis near the sternal carina (Dial, 1992). A small (approximately 15mm) incision was made on the antero-dorsal aspect of the shoulder in order to expose and clean the dorsal surface of the delto-pectoral crest (DPC) for attachment of the strain˙gauge. This requires minimal disruption of the muscles (primarily the deltoid) attaching on the dorsal surface of the DPC. The deltoid muscles were retracted and the DPC was lightly scraped with a scalpel blade to remove the periosteum. After defatting and drying the bone surface, a strain gauge was bonded to the bone's surface using a self-catalyzing cyanoacrylate adhesive. In three of the birds, a single-element metal foil strain gauge (type FLG-02-11, Tokyo Sokki Kenkyujo, Ltd,

Tokyo, Japan) was used. In the fourth bird, a rosette strain gauge (type FRA-1-11) was bonded to the DPC (Fig. 1), so that the principal axis of strain produced by the pectoralis could be determined (Dally and Reilly, 1978). Single-element strain gauges were attached perpendicular to the axis of the humerus in the presumed direction of tensile principal strain produced by the pull of the pectoralis. This direction also makes the strain gauge minimally sensitive to strains produced by aerodynamic and muscular forces transmitted along the bone's shaft, which are estimated to be less than 6% of pectoralis-generated strains (N=20), based on hand manipulation of the humerus to simulate the bending, compression and torsion of its shaft that might occur due to its loading during flight.

By projecting anteriorly from the proximal shaft of the humerus, the DPC effectively forms a short cantilever. In pigeons, as well as starlings (Biewener *et al.* 1992), nearly the entire insertion area of the pectoralis aponeurosis is onto the ventral surface of the DPC, rather than the shaft of the humerus. Because of this, when the pectoralis muscle contracts to generate tension against its (ventral) undersurface, the DPC is bent downward. This produces mainly tensile strain on the dorsal surface of the DPC, perpendicular to the longitudinal axis of the humerus. In combination with the nearly linearly elastic mechanical behavior of vertebrate bone over a wide frequency range of loading (up to 100Hz, Lakes *et al.* 1979; the natural frequency of strain vibration recorded in a goat tibia is greater than 700Hz, K. P. Dial and A. A. Biewener, unpublished results), this makes the DPC an excellent skeletal 'force-transducing process'. In the starling (Biewener *et al.* 1992), we estimated the error due to the potential hysteresis between applied force and the resulting deformation of the bone to be less than 1% of measured force.
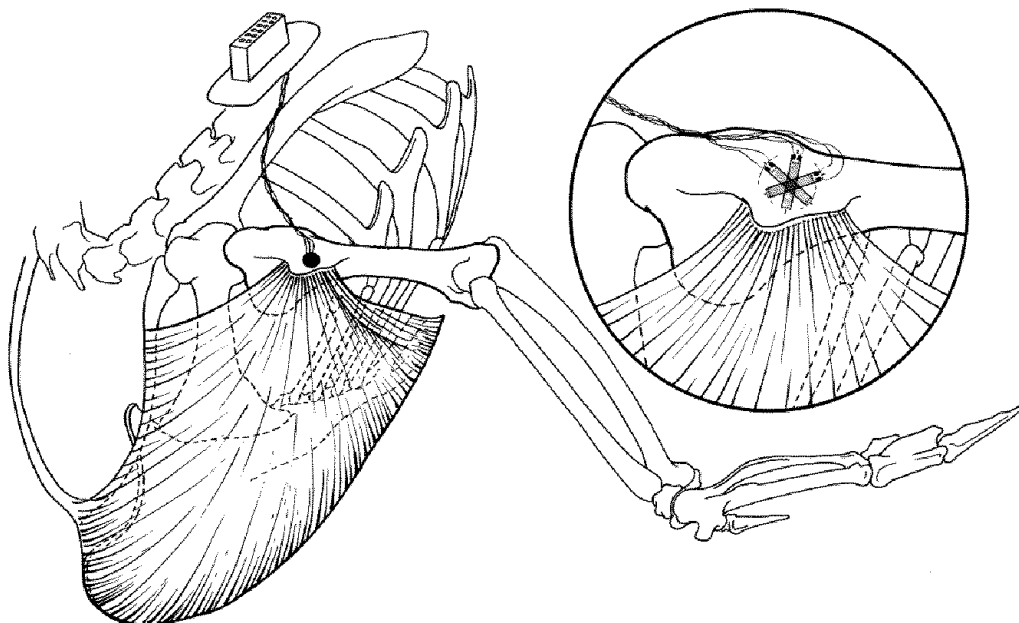

Fig. 1. An oblique antero-dorsal view of the left shoulder of the pigeon (*Columba livia*) showing the position of a rosette strain gauge attached to the dorsal surface of the deltopectoral crest (DPC) of the humerus. Magnified circular inset shows approximate orientation of the three strain gauge elements of the rosette as they were aligned during recording.

The strain gauge lead wires (36 gauge, Teflon-coated) were passed underneath the deltoid muscle and over the shoulder to a custom-designed connector (back-plug, Microtech, FM-6) mounted on the animal's back (Fig. 1). The back-plug was anchored to the animal by suturing its base to intervertebral ligaments, and the skin was sutured tightly around the base of the plug and sealed with a silicone rubber adhesive (Dow Corning).

In addition to the strain gauge, a bipolar, indwelling electromyographic (EMG) electrode (0.1mm diameter, 99.9% silver, enamel-insulated wire, 0.5mm intertip distance) was threaded subcutaneously from the dorsal back-plug to a ventral site over the pectoralis near the sternal carina and implanted (using a 25 gauge hypodermic needle) in this portion of the muscle (sternobrachialis or SB, Dial *et al.* 1988). A shallow loop (approximately 5–10mm in length) was formed from the portion of the electrode exiting the muscle and sutured to the ridge of the carina so that the implanted electrode could move freely with the contracting muscle, thereby reducing movement artifact in the EMG signal. All skin incisions were kept moist during surgery and sutured closed following implantations. During recovery from surgery, the birds were fitted with protective, cone-shaped collars and placed in a recovery cage supplied with water, food and a heated pad.

All flight recordings were made the day following surgery. Pectoralis EMG and DPC strain (single-element or rosette strain gauge) signals were transmitted from the animal to the amplifier equipment by means of a lightweight shielded cable (30m long) connected to the backplug of the bird as it flew down the hall. The cable shielding was grounded to the bird's skin. Strain signals were amplified (1600 times) *via* a conditioned Wheatstone bridge circuit (Vishay model 2120, Micromeasurements). EMG signals were amplified (1000–5000 times) and filtered (100–3000Hz half-amplitude band pass and 60Hz notch filter) using Grass P511J preamplifiers. EMG and DPC strain signals were recorded, together with a synchronization pulse from the camera's shutter, onto FM tape (Hewlett-Packard, model 3694A) and simultaneously sampled *via* an analog-to-digital converter (Keithley Instruments series 500) at 2040Hz and stored on computer.

Digital data were analyzed on a Tektronix 4109 graphics terminal using software provided by G. V. Lauder. EMG onset, duration and intensity (determined by calculating the area under each rectified signal) were calculated for each wingbeat cycle chosen for analysis. Permanent copies of the experimental recordings were printed using a Gould (2400) pen-recorder.

After flight recordings, the DPC strain outputs were calibrated to force following a similar procedure described by Biewener *et al.* (1992). In two of the birds, the maximum isometric force of the pectoralis was determined *in situ* by supramaximally stimulating (0.1ms pulse duration at 100Hz, for a total duration of 1s) the rostral and caudal pectoral nerves. These nerves were exposed dorsally. Silver bipolar electrodes were attached and isolated by sheathing the nerves and electrodes in Silastic tubing (Dow Corning). The humerus was left intact at the shoulder in an attempt to simulate mechanical loading of the DPC during flight. A short length of silk suture (compliance: $0.045\,\text{mN}^{-1}\,\text{cm}^{-1}$) was tied around the distal end of the humerus and connected to the isometric force transducer (Grass, model FT10). The thoracic vertebrae of the bird were clamped to a frame and the sternal keel was anchored to a brace positioned underneath the animal. The muscle's

length was adjusted (by means of humeral elevation) until peak twitch tension was obtained, prior to making measurements of tetanic force. Strain output from the DPC gauge was recorded simultaneously to obtain a tetanic calibration of muscle force. In all four birds, DPC strain was also calibrated to muscle force *insitu* by pulling directly on the pectoralis by means of a silk suture (tied about the muscle's tendinous insertion below the DPC) connected to the force transducer. Measurements were made at 10° intervals of humeral elevation, ranging from horizontal to 70° above horizontal. This corresponds to most of its range of movement during flight. In all positions, the humerus was protracted 60° from the vertebral axis, as it is during flight.

A dynamic calibration of DPC strain in relation to force was obtained by digitally sampling the signals from the force transducer and the strain gauge and fitting a reduced major axis (model II) regression to the rise and the fall in force (Fig. 2). We obtained linear fits of the data ($r^2=0.996\pm0.006$, $N=20$), with 95% confidence intervals of the regression that were less than 4% of the calibration slope.

Principal strain calculations

In the case of bird D, in which a rosette strain gauge was attached to the DPC, the maximum and minimum principal strains and their orientation to the DPC were computed from digitized raw strains recorded from the three strain gauge elements (ϵ_1, ϵ_2 and ϵ_3) of the rosette strain gauge; the largest (absolute magnitude) principal strain being the strain that corresponds to the primary axis of loading. If the DPC functions as a 'cantilever', as we propose, the maximum principal strain on its dorsal surface is expected to be tensile (positive) and oriented generally along the axis of the DPC, perpendicular to the humeral shaft. As noted above, we assumed this loading scheme in earlier experiments when using single-element strain gauges attached to the DPC. The purpose of making rosette strain
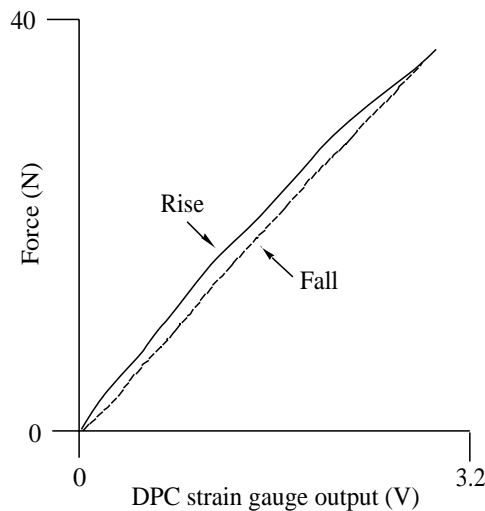

Fig. 2. Representative calibration curve for the rise and fall in tetanic muscle force (N) *versus* DPC strain output (V). Dynamic calibrations such as this were obtained by digitally sampling the two outputs and employing a reduced major axis regression. The mean correlation coefficient of these calibrations in all four birds was 0.996 ($N=20$); 95 % confidence intervals were less than 4 % of the calibration slopes.

recordings in this bird was to verify this assumption and to delimit the principal strain axis for future studies using single-element gauges.

Muscle fiber measurements

In order to estimate the fiber area of the pectoralis for the purposes of determining average muscle stress, we measured fiber (fascicle) length and fiber angle (with respect to the muscle's central tendon, the membrana intermuscularis) at 10mm intervals on both the deep (N=10) and superficial (N=12) aspects of each muscle. Recent work has shown that the pectoralis of certain avian species and certain mammalian muscles are composed of shorter serially interdigitated fibers (Gaunt and Gans, 1990; Trotter *et al.* 1992), rather than a single fiber that runs from end to end within a fascicle. Hence, the lengths that we measure are those of the fascicle and not necessarily those of the fibers. Given that this does not affect our interpretations of overall force development and percentage length change, we do not make a distinction between fiber length *vs* fascicle length. In general, fiber fascicle length ranged from 24 to 63mm, with a mean of 42±16mm. Fiber angle ranged from 5 to 40°, with a mean of 23±11°. We used mean fiber length and fiber angle to calculate muscle fiber area according to the method of Alexander (1977), assuming a muscle density of 1060kg m^{-3}.

The pigeon pectoralis is largely composed of fast oxidative muscle fibers (84–94%), with considerably fewer glycolytic fibers (6–16%) (Kaplan and Goslow, 1989; Rosser and George, 1986; Talesara and Goldspink, 1978). However, it would be misleading to associate these oxidative or 'red' fibers with the slow twitch (Type I, or SO 'slow oxidative') fibers typical of mammals, given the high wingbeat frequency and the presumably fast shortening velocity of this muscle in the pigeon. The strong staining for both oxidative enzymes and a high myosin ATPase activity (Talesara and Goldspink, 1978) suggest that these fibers are best characterized as being fast oxidative. Because a considerable volume of these oxidative fibers is composed of non-contractile components (mitochondria: 30%, James and Meek, 1979; capillaries: 10%, estimated from the data of Conley *et al.* 1987), we estimated the myofibrillar cross-sectional area of the pectoralis by subtracting the area fractions of these components from the overall fiber areas calculated for the muscle as described above.

Results

Principal strains and strain orientation in the DPC

Raw strains (ϵ_1, ϵ_2 and ϵ_3) recorded from individual elements of the rosette gauge attached to the DPC of bird D are shown (Fig. 3B), together with the principal strains (ϵ_{max} and ϵ_{min}) and the angle (ϕ) of ϵ_{max} to the antero-posterior axis of the DPC (Fig. 3C) computed from the raw strains, for three successive wingbeats. Over the time when force development is near a peak level (>50% of maximum), the orientation of maximum (tensile) principal strain is aligned along the antero-posterior axis of the DPC, ranging from +5 to −20° relative to this axis. This is the orientation of tensile strain expected for the DPC being bent downward by the pull of the pectoralis, perpendicular to the shaft of
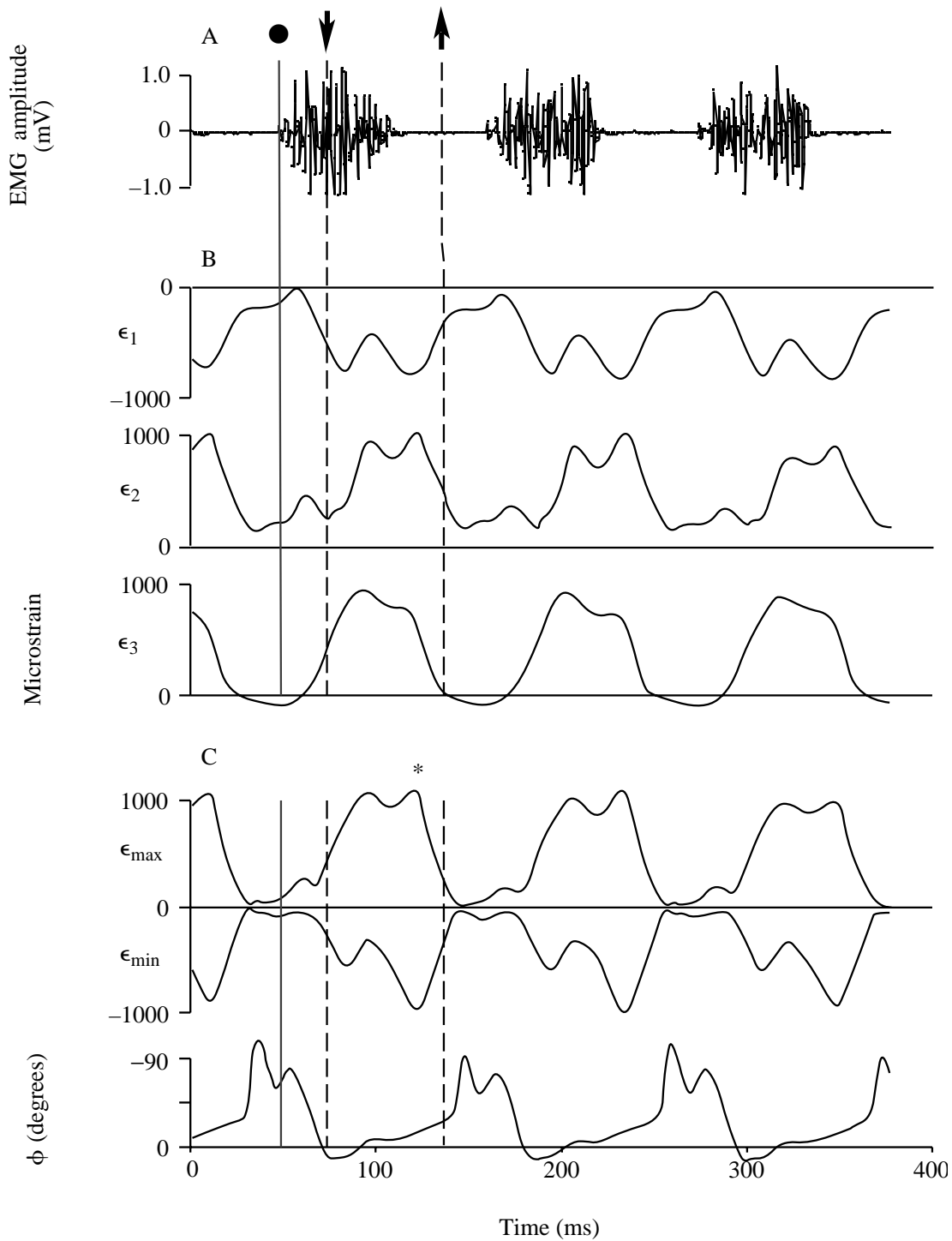
Fig. 3. (A) Simultaneous *in vivo* electromyographic (EMG) signals from the pectoralis muscle and (B) rosette strain gauge recordings (ϵ_1, ϵ_2, ϵ_3) from the DPC of three wingbeat cycles during level flapping flight. ● denotes EMG onset during the end of the upstroke, the downward arrow denotes the start of the downstroke and the upward arrow denotes the start of the upstroke. (C) Maximum (ϵ_{max}) and minimum (ϵ_{min}) principal strains together with the orientation (ϕ) to the DPC axis computed from the digitized rosette strain signals in B above. * denotes the point of maximum principal strain during the downstroke, which is depicted in Fig. 4 as a tensile vector. Note that ϕ is plotted from 0° to −90°.

the humerus (Fig. 4). During the entire period of force generation by the muscle, the orientation of principal strain shifts approximately 40° (represented by the stippled wedge in Fig. 4), tending to be oriented more proximally at later stages of the downstroke. The large excursions in principal strain angle during the upstroke are expected and probably reflect the effect of smaller forces transmitted to the DPC by wing elevators (when strain is quite low) which affect the orientation and, less significantly, the magnitude of strain. Note that when the pectoralis begins to contract (EMG in Fig. 3A), exerting tension on the undersurface of the DPC (increase in ϵ_{max} in Fig. 3C), the angle (ϕ) of maximum principal strain rapidly shifts to become aligned just antero-distally (+15°) to the DPC axis. Hence, these data confirm the reliability of using single-element strain gauge recordings of the DPC to transduce pectoralis force *in vivo*.

Pectoralis force and EMG versus *mode of flight*

A qualitative relationship between the raw EMG amplitude and the force output of the pectoralis is immediately evident from a composite flight recording, which shows the animal taking off from the ground, flying level for 20m, and landing on a perch at the end of the hallway (Fig. 5). Detailed sequences of each of these three phases of flight are shown in the following figures (Figs 6–9), together with those during vertical ascending (Fig. 10) and descending (Fig. 11) flight. Peak forces recorded for five wingbeats of each of the four birds were averaged ($N=20$) to compare peak force levels among the different modes of flight.
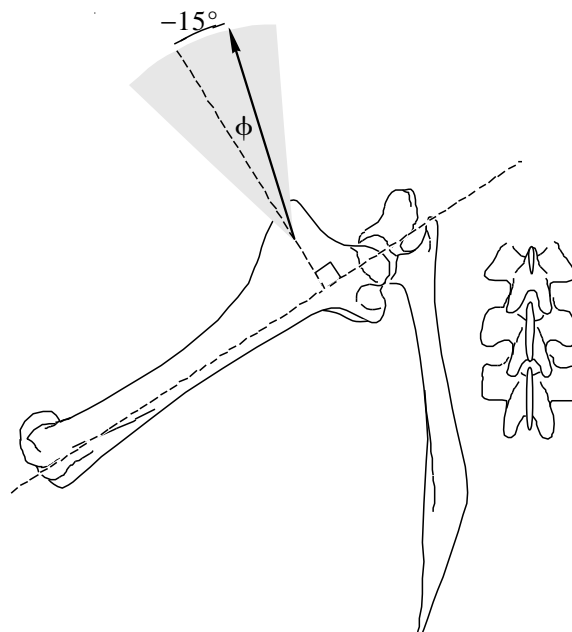

Fig. 4. Dorsal view of the left shoulder (humerus, scapula and several thoracic vertebrae) of the pigeon showing the orientation of principal tensile strain generated by the pectoralis muscle in the dorsal surface of the delto-pectoral crest during the downstroke. Rosette strain recordings showed that at maximal force development the orientation of principal strain was −15° (proximo-anterior) to the perpendicular axis of the DPC (vector corresponds to the asterisk in Fig. 3C). The orientation of ϵ_{max} varied from +15 to −25° (stippled wedge) relative to the DPC axis during the downstroke.

Takeoff

Immediately prior to lift-off (the initial half of the first EMG burst during takeoff, Fig. 6), as the wing is first elevated and the pectoralis is being stretched, the force generated by the pectoralis rises but then falls transiently at the onset of the downstroke. This transient decay in force corresponds to a distinct biphasic EMG burst and may reflect
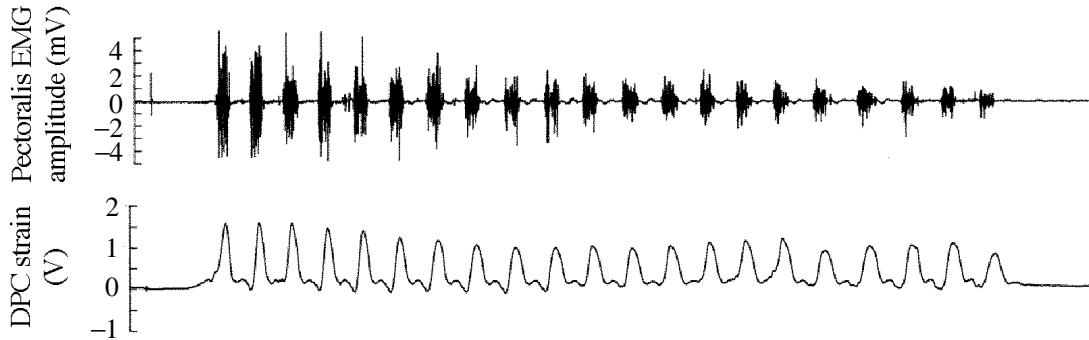

Fig. 5. Simultaneous electromyographic signals from the pectoralis and tensile strain obtained from a single-element strain gauge attached to the dorsal delto-pectoral crest (DPC) of bird B during a ground takeoff, brief level flight and landing on a perch platform. Note the correlation of EMG amplitude and intensity to peak DPC strain.
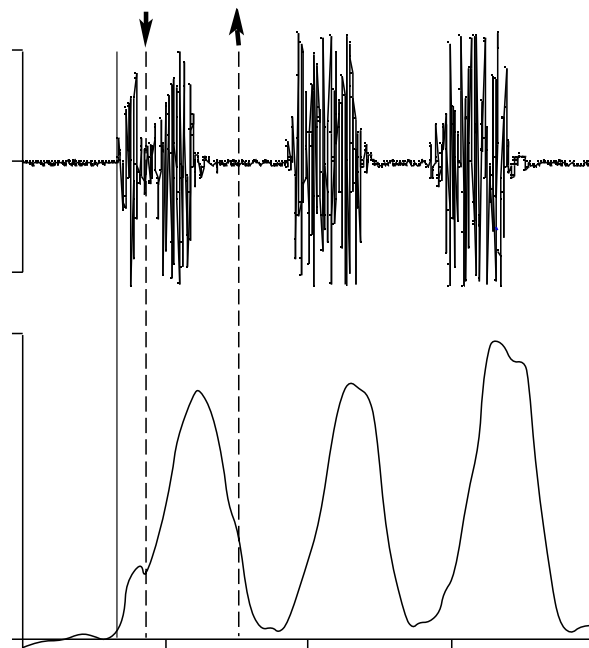

Fig. 6. Representative pectoralis EMG and single-element bone strain/muscle force recordings during takeoff in relation to the kinematics of the first of the three wingbeat cycles shown above (● denotes EMG onset, the downward arrow denotes the start of the downstroke, and the upward arrow denotes the start of the upstroke). Note that the bird is still on the ground elevating its wings from ● to the downward arrow and that lift-off occurs during the first downstroke (downward arrow). See text for further explanation.

the fact that the bird is still on the ground during this initial upstroke–downstroke transition, as the muscle shifts from active lengthening to shortening. Both the brief increase and transient decay in force and the distinct biphasic bursting pattern of the EMG are absent in the subsequent wingbeats once the bird is airborne. Instead, pectoralis force rises smoothly during wing turn-around and the EMG signal maintains a fairly uniform amplitude. Force production commences 310ms after the EMG onset (labelled ● in Fig. 6) and reaches a peak midway through the downstroke. Peak muscle force averaged 24.9±3.1N during the takeoff phase of flight. Since the legs thrust the bird upward during lift-off, the highest recordings of pectoralis force and EMG intensity (mV×ms) is observed during the second or third wingbeat. Pectoralis force is sustained well after the cessation of EMG activity, being maintained throughout the downstroke. Force does not fall to zero until about 15ms after the beginning of the upstroke, indicating significant antagonistic activity with the supracoracoideus (and possibly deltoideus), the major wing-elevating muscle. Wingbeat frequency averaged 9.0±0.3Hz (*N*=40) during takeoff.

Level flight

   During level flapping flight (Fig. 7), very consistent strain profiles of pectoralis force were recorded from the DPC for successive wingbeats. As for the airborne phase of takeoff, muscle force rises smoothly during the latter third of the upstroke (from the ● to the downward arrow in Fig. 7), as the muscle is being stretched, with a slight change in
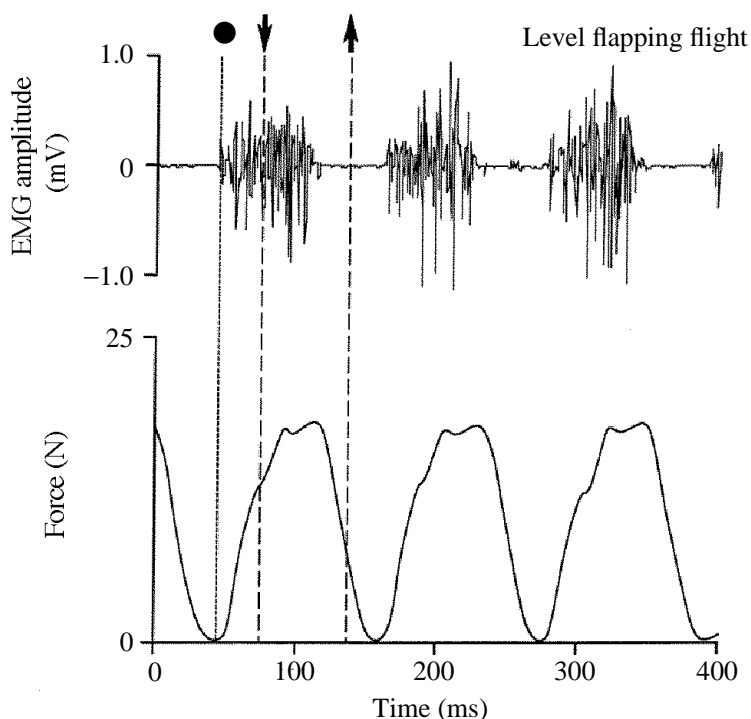

Fig. 7. Representative pectoralis EMG and bone strain/muscle force recordings during level flight (approximately $8\,\mathrm{ms}^{-1}$) in relation to the kinematics of the first of the three wingbeat cycles shown above (notation of symbols and arrows as in Fig. 7). Highly consistent recordings such as this were obtained for all individuals during level flight.

slope evident as the wing begins to move back down. In contrast to the takeoff phase, however, muscle force peaks earlier in the downstroke but is still maintained well beyond the beginning of the upstroke (Fig. 8). Average peak force recorded during level flight was 19.7±2.0N in the four birds at an average wingbeat frequency of 8.6±0.3Hz (N=40). Forward flight velocities ranged from 6 to 9 m s^{-1}.

Landing

During landing (Fig. 9), force developed by the pectoralis diminished gradually in successive wingbeats until the bird alighted on the landing platform. Peak forces averaged 18.7±2.5N (N=40) during landings, falling to as low as 5N in the final wingbeat. Moreover, peak force occurs earlier in the downstroke, compared to takeoff and level flight, reaching zero prior to the subsequent upstroke. This suggests that by being activated earlier in the wingbeat cycle the pectoralis performs more negative work during landing, as shown by the greater area under the force recording during the upstroke as the bird lands. Because we were unable to obtain adequate films to evaluate the kinematics of the wing during landing (which is more complex than that during level flight), we cannot document this increase in negative work. Consistent with the decline in muscle force, the amplitude of the EMG also diminishes in a stepwise fashion during the final three wingbeats as the bird lands (Fig. 9). During landing flight, wingbeat frequency averaged 8.0±0.6Hz (N=40).
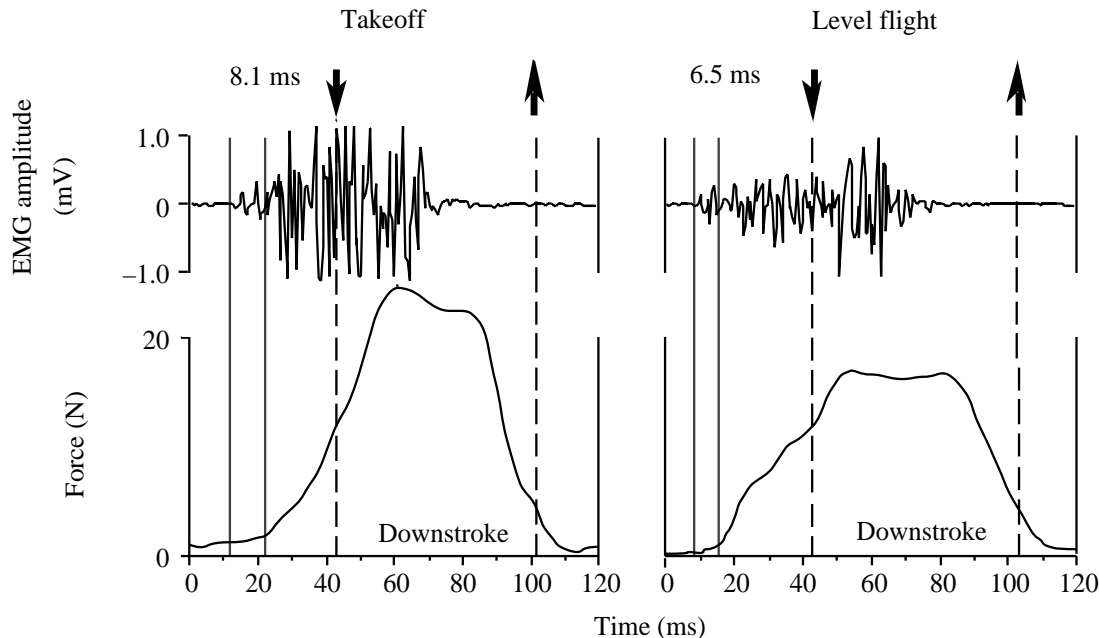

Fig. 8. Expanded recording of pectoralis EMG and muscle force for a single wingbeat cycle during takeoff and level flapping flight showing that the pectoralis develops force during the latter one-third of the upstroke. The latencies of force relative to the onset of their EMGs in these two samples are 8.1ms for takeoff and 6.5ms for level flapping flight. Maximum force is developed during the first third of the downstroke for both modes of flight. The duration of muscle force (approximately 80–90ms) exceeds the duration of the EMG (50–60ms), lasting throughout the entire downstroke.
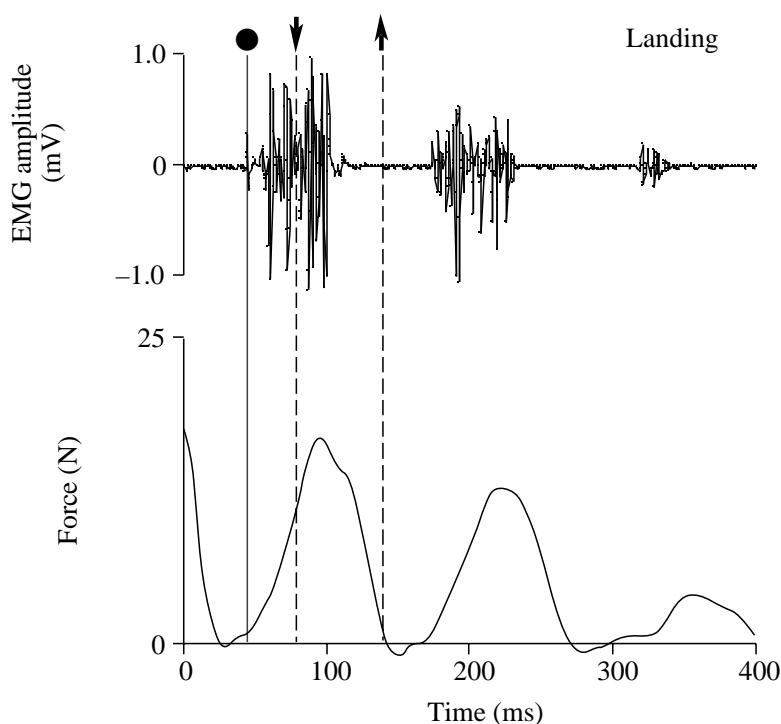
Fig. 9. Representative pectoralis EMG and bone strain/muscle force recordings during landing in relation to the kinematics of the first of the three wingbeat cycles shown above (notation of symbols and arrows as in Fig. 7). In contrast to the situation in takeoff and level flight, pectoralis force relaxes to zero by the end of the downstroke.

Vertical ascending flight

The largest forces that we recorded were developed during vertical ascending flight, with peak forces averaging 26.0±1.8N (*N*=40). The highest wingbeat frequencies were also observed during vertical ascending flight, averaging 9.1±0.3Hz (*N*=40). Otherwise, the general profile of muscle force development in relation to the EMG and the timing of the upstroke and downstroke are quite similar to those during level flight. The main difference is that, during vertical ascending flight, muscle force rapidly diminishes to near zero at the beginning of the upstroke (Fig. 10), presumably decreasing the degree of antagonistic activity between the pectoralis and the supracoracoideus.

Descending flight

Surprisingly, peak forces developed during near-vertical descending flight were significantly larger than those recorded during level flight, averaging 23.7±2.7N (*N*=40). The force profiles among successive wingbeats are more variable than during the other modes of flight (Fig. 11). This is probably due to the fact that the bird's body swings through an approximately 90° arc about the shoulder, having been released from the hand in a horizontal position and shifting to land with its body in a more vertical orientation on the platform. During descending flight, wingbeat frequencies averaged 8.8±0.5Hz (*N*=40).
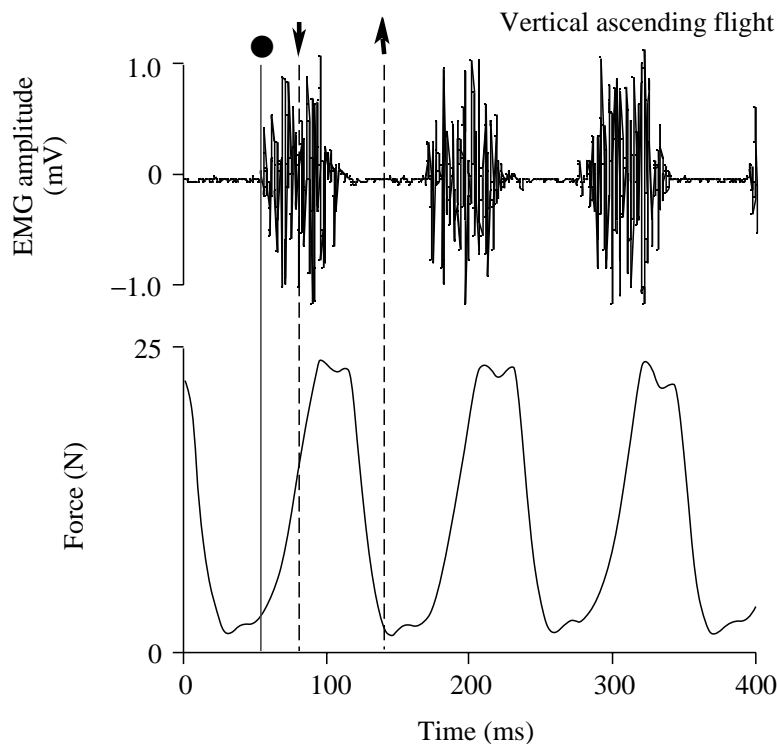
Fig. 10. Representative pectoralis EMG and bone strain/muscle force recordings during vertical ascending flight (about a 2.5m climb) in relation to the kinematics of the three wingbeat cycles shown above (notation of symbols and arrows as in Fig. 7). Peak forces reach about 26N, which is the maximum force output for all modes of flight. Pectoralis force relaxes to zero by the end of the downstroke.

Loaded-flight experiments

When harnessed with a weighted backpack, the maximum weight that two of the birds could carry and independently take off from the ground was approximately 50% (150g) of their body weight (BW). Peak forces generated by the pectoralis during level flight while carrying this additional load averaged 21.9±2.8N (N=20) (Fig. 12B). Peak forces developed during takeoff with the weighted backpacks averaged 25.8±1.1N (N=20). Correspondingly, the maximum load that either bird could carry and sustain level flapping flight (after being gently tossed into the air) was 100% of BW (300g). When subjected to this weight, however, the birds could not take off from the ground by themselves nor could they land on the perch at the end of the hall. Peak forces, developed when flying with a total 'cargo' of twice BW, averaged 26.4±0.7N (N=20) (Fig. 12B). Hence, relative to normal unloaded level flight, pectoralis force increased by 18% when the birds flew with a 50% increase in BW and by 42% with a 100% increase in BW.

Overall, the maximum forces developed by the pectoralis during these differing modes of flight (Fig. 12A) and when carrying loads on their back of up to 100% BW (Fig. 12B) did not exceed 27N, which is well below the maximum isometric force (67N) that this muscle is capable of generating. Isometric force was determined by averaging the *in situ* isometric force measured in two of the birds (67.7 and 61.3N) with that estimated from mean myofibrillar cross-sectional area of the four muscles (Table 1), assuming a peak
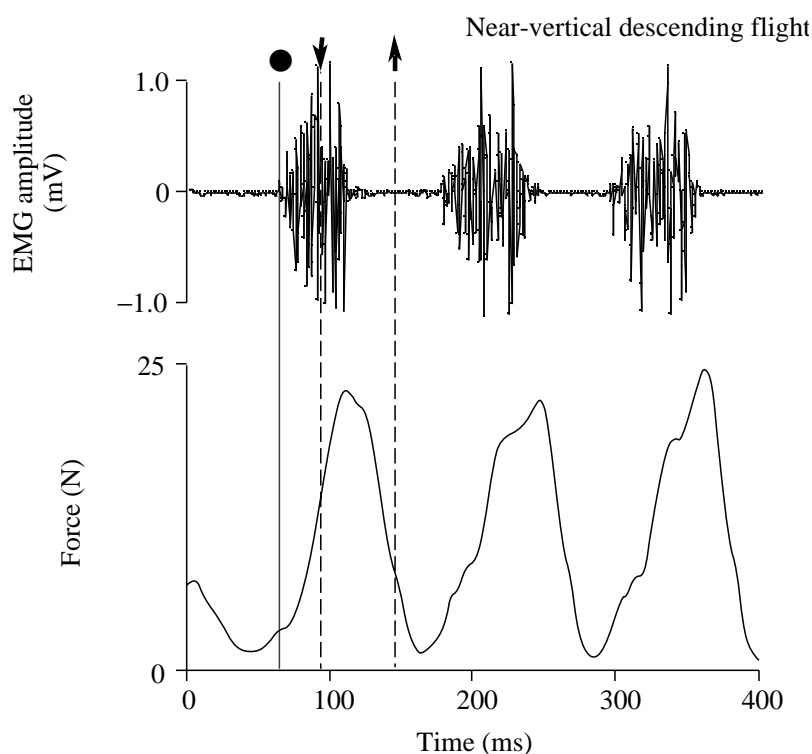
Fig. 11. Representative pectoralis EMG and bone strain/muscle force recordings during near-vertical descending flight in relation to the kinematics of the first of the three wingbeat cycles shown above (notation of symbols and arrows as in Fig. 7).
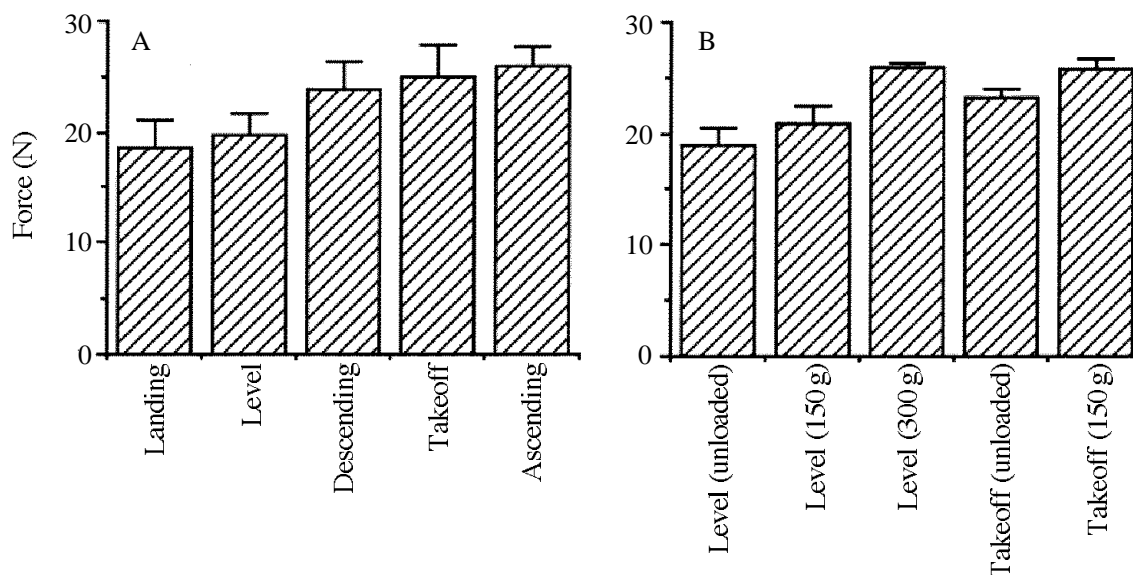

Fig. 12. (A) Summary of the peak forces (N) generated by the pectoralis muscle during five modes of free flight (4 birds, 10 wingbeat cycles analyzed per flight mode per bird). Note the relatively narrow range of forces (18–26N) exhibited during these very different flight modes. (B) Comparison of peak forces generated by the pectoralis muscle in pigeons carrying a weighted backpack (150g and 300g) during level flight and takeoff (150g) (2 birds, 10 wingbeats analyzed per mode per bird). Note that maximum peak forces generated during loaded flight did not significantly exceed forces generated during unloaded vertical ascending flight. Bars show 1 s.e.

Table 1. *Morphological measurements of the pigeon pectoralis*

Pigeon	Body mass (g)	Pectoralis mass (g)	Fiber length (mm)	Pinnation angle (degrees)	Area (cm^2)	*Estimated myofibrillar area (cm^2)	Moment arm, r (mm)
A	301	28.8	39.3±11.9	35	5.66	3.40	8.5
B	311	33.9	43.6±15.8	32	6.15	3.69	7.9
C	314	31.8	44.5±12.4	35	5.52	3.31	10.2
D	301	28.0	38.0±10.7	37	5.55	3.33	8.0

*Calculated according to Alexander (1977), assuming a muscle density of 1060kgm^{-3}.
Values for fibre length are mean ± S.D., N=10–12.

isometric stress of 200kPa for vertebrate skeletal muscle. The range of muscle force output among these broad flight conditions, therefore, is surprisingly narrow, with muscle force increasing by only 41% from landing (18.7N) to when the birds flew with a 100% BW load (26.4N), or when they ascended in vertical flight (26.0N). These latter two flight conditions probably reflect what is almost the maximum performance capability of the birds. Based on a mean myofibrillar cross-sectional area of 3.43cm^2 for the pectoralis of the four birds, the peak stresses developed during each mode of flight are: takeoff, 73kPa; level flight, 57kPa; landing, 54kPa; ascending, 76kPa; and descending, 69kPa. When flying level and carrying a 100% BW load, peak stress developed by the pectoralis was 77kPa.

Muscle work and power output

The force developed by the pectoralis muscle in relation to changes in fascicle length for one contraction cycle of pigeon C during level flight and during takeoff is shown in Fig. 13. Length changes of the muscle's fibers were calculated based on the moment arm (r) of the pectoralis at the shoulder (measured as the distance from the center of the muscle's attachment on the DPC to the center of rotation of the humerus at the shoulder, Table 1), the orientation of the muscle's fibers arising from the keel of the sternum with respect to the shoulder joint, and measurements of the angular displacement of the humerus obtained from high-speed light ciné films taken of the animal in anterior view as it flew down the hall. Given the very short tendinous insertion of the pectoralis onto the ventral surface of the DPC, measurements of overall (muscle–tendon) length change determined from angular displacements of the humerus are probably close to those of the muscle's fibers themselves. In this bird, muscle fiber fascicle length averaged 44.5±12.4mm (Table 1). Consequently, the changes in muscle length shown in Fig. 13 are calculated relative to its mean resting length (determined after the muscle had been removed from the animal). The angular excursion of the humerus during level flight is about 82°, moving from 62° above horizontal at the beginning of the downstroke to 20° below horizontal at the end of the downstroke. During takeoff, angular excursion of the humerus increases to 141° (from 90° above horizontal to 51° below horizontal).

The open area within each counter-clockwise loop represents the net work done by the
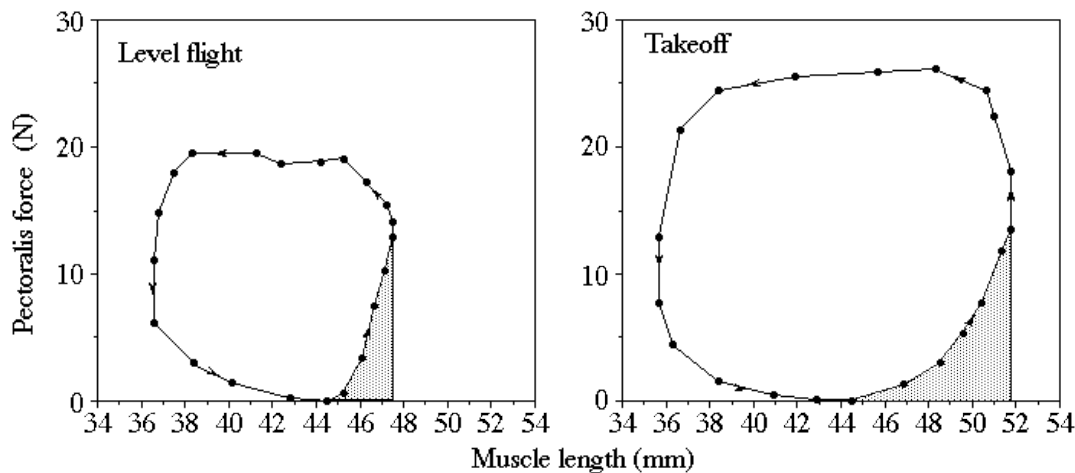
Fig. 13. Comparison of calculated 'work-loops' during level flapping flight and takeoff. Force developed by the pectoralis of a pigeon during level flapping flight and takeoff are plotted against changes in average pectoralis fiber (fascicle) length for a single wingbeat cycle. Individual points represent values of muscle length change determined from wing kinematics at 23 time increments (5ms apart) for level flight and 22 time increments for takeoff, normalized as a fraction of the contraction cycle and correlated with values of force determined at corresponding time intervals. Resting (unloaded) length is assumed to be 44.5mm, the average length of the pectoralis muscle fibers of bird C. The shaded region indicates negative work performed by the muscle when it is stretched by the wing's inertia during the final third of the upstroke. The unshaded region contained within the loop represents the net positive work performed by the muscle in one contraction cycle. Overall shortening of the muscle corresponds to a fiber strain of 25% during level flight and 37% during takeoff.

muscle during a single contraction cycle (Fig. 13). The shaded region indicates the negative work absorbed by the muscle as it is stretched to decelerate the wing at the end of the upstroke. The total area under the curve (shaded plus unshaded) represents the positive work performed by the muscle during the downstroke to power level flight. Because force developed by the pectoralis does not fall to zero by the end of the downstroke during level flight and takeoff (Figs 6, 7 and 8), some positive work is lost as the muscle is forcibly re-extended at the beginning of the upstroke, presumably by its major antagonist, the supracoracoideus. Indeed, our recordings indicate that the pectoralis relaxes to zero force only briefly during the wingbeat cycle for most of the flight conditions that we examined.

During level flight, negative work is small (15mJ) as activated muscle fibers are stretched by 3.2mm (7% strain). The muscle fibers subsequently shorten by an average of 11.1mm, corresponding to a fiber strain of −25%, to perform a total of 189mJ of positive work. During takeoff from the ground (the third wingbeat is shown), both negative work (32mJ) performed to decelerate the wing (+16% fiber strain) and total positive work (421mJ, −37% fiber strain) are much higher. Net shortening of the fibers after being stretched is 21%. The average shortening velocity of the pectoralis is 4.4lengths s^{-1} during level flight and 6.7lengths s^{-1} during takeoff. By multiplying these values of work times the bird's wingbeat frequency in each case, we can obtain estimates

of the average power output of the pectoralis (and hence the whole animal) over a wingbeat cycle for each of these flight conditions. This calculation ignores contributions of other wing muscles to the animal's total power output, but these are likely to be small in comparison. As both pectoralis muscles are active to generate power, this yields 3.25W during level flight (8.6Hz) and 7.59W during takeoff (9.0Hz) for the power output of the whole animal. Correspondingly, the mass-specific power output of the pectoralis muscle is $51\,\mathrm{W\,kg^{-1}}$ during level flight and $119\,\mathrm{W\,kg^{-1}}$ during takeoff.

When ascending vertically to the higher (2.5m) landing perch, the pigeons' average steady rate of climb measured from film was $2.62\,\mathrm{m\,s^{-1}}$. At this velocity, therefore, the pigeons climbing power (mean body weight: 3.1N) is 8.12W. This 'whole-animal' measure of power output compares well with the slightly lower value that we calculate above based on our measurements of pectoralis force and estimates of muscle fiber length change.

Discussion

The mass-specific power output that we calculate from our direct recordings of force and estimates of fiber shortening of the pigeon pectoralis during moderate speed level flight ($51\,\mathrm{W\,kg^{-1}}$ at about $8\,\mathrm{m\,s^{-1}}$) is substantially lower than that ($110\,\mathrm{W\,kg^{-1}}$ muscle) predicted by Pennycuick (1968, 1975) for a pigeon flying at the same speed on the basis of fixed-wing aerodynamic theory. Our empirical results, therefore, indicate that non-steady mechanisms for generating lift and thrust during flapping flight, such as changes in wing shape, require considerably less power in birds than that predicted by quasi-steady aerodynamic theory. The maximum specific power output that we measure for the pigeon pectoralis ($119\,\mathrm{W\,kg^{-1}}$ muscle) is also well below the theoretical maximum sustained power output of $250\,\mathrm{W\,kg^{-1}}$ muscle derived by Weis-Fogh and Alexander (1977), based on estimates of the maximal stress-generating capability and intrinsic speed of shortening of striated muscle.

Some caution in our empirical measurements is also warranted, given the limitations of our method for calibrating the DPC strain recordings to muscle force. Our method requires that the wing be held in a fixed position as force is developed by the muscle *via* synchronous stimulation. Neither of these conditions is met during the actual activation (K. P. Dial and D. F. Boggs, in preparation) and development of force by the pectoralis during flight. The change in humeral orientation during the upstroke and downstroke, when the pectoralis is active, results in a 15% variation in force calibration relative to DPC strain (the change in principal strain angle during force development is one likely source of this variation). These limitations in methodology, which are unavoidable, may lead, to some extent, to our underestimating maximal force and power output using this approach.

Using the same method as the present one for pigeons, we recently measured $104\,\mathrm{W\,kg^{-1}}$ muscle for the pectoralis of a starling flying at about $14\,\mathrm{m\,s^{-1}}$ in a wind tunnel (Biewener *et al.* 1992). Because of its smaller size (72 *vs* 310g) and generally higher wingbeat frequency, a starling would be expected to have a higher mass-specific muscle power output compared to a pigeon at comparable levels of performance. Hence,

the values we obtain for these two species operating at different flight performance levels compare well. The value of $119\,W\,kg^{-1}$ muscle we obtain for maximal mass-specific power output of the pigeon pectoralis also compares favorably with estimates of induced power output obtained by Marden (1987) for a wide range of flying birds and insects lifting maximal loads and re-analyzed for estimates of mass-specific muscle power by Ellington (1991). These data show a range of $111–177\,W\,kg^{-1}$ muscle for birds ranging in size from 10 to 920g. Finally, our empirical measurements of maximal power output in the pigeon also compare favorably to those obtained *in vitro* for synchronous muscles of insects ($76–90\,W\,kg^{-1}$ muscle; Josephson, 1985; Stevenson and Josephson, 1990). Based on oxygen consumption measurements obtained for pigeons flying in a wind tunnel, Rothe and Nachtigall (1987) show that a pigeon consumes about $106\,W\,kg^{-1}$ bodymass when flying at a speed of $8\,m\,s^{-1}$. Combining our estimate of mass-specific whole-animal mechanical power output at this speed ($10.5\,W\,kg^{-1}$ bodymass) yields an overall flight efficiency of 10%. This is slightly lower than the flight efficiency of the European starling, which was calculated to be 13% when flying at about $14\,m\,s^{-1}$ (Biewener *et al.* 1992). Rothe and Nachtigall (1987) observed a minimum metabolic cost ($100\,W\,kg^{-1}$ bodymass) at about $11\,m\,s^{-1}$ in their pigeons, suggesting that a higher flight efficiency might be obtained at this higher speed. Locomotor efficiencies of similarly sized terrestrial mammalian and avian taxa are comparable (Heglund *et al.* 1982), but our values of flight efficiency fall below estimates of the partial efficiencies of flying birds (19–30%; Tucker, 1972; Bernstein *et al.* 1973) and bats (19–27%; Thomas, 1975).

Range of muscle force and power output as a function of flight performance

Probably the most interesting and important finding of our study is that the maximal force production of the pigeon pectoralis spans only a narrow range relative to what would otherwise appear to be quite a broad range of flight performance. Peak stress (or force) in the pectoralis increases by only 41% from landing flight to vertically ascending flight, ranging from 54 to 76kPa. Even when the birds flew carrying an additional 300g (100% BW) load, peak muscle stress did not exceed 77kPa. Vertically ascending flight and maximum load carrying each probably represent maximal power output requirements of the animal's flight musculature. Under these conditions, however, the highest forces (stresses) developed by the pectoralis are only about 39% of isometric values (Fig. 14A).

This narrow range of maximal force generation is in sharp contrast to the range of muscle stresses recorded in the ankle extensors of kangaroo rats (*Dipodomys spectabilis*) during hopping and jumping (Biewener *et al.* 1988). In kangaroo rats, peak muscle stresses range nearly fourfold, from 85 to 360kPa (Fig. 14B), over this performance range. At the highest jumps recorded, peak forces generated by the kangaroo rat's ankle extensors exceeded their peak isometric force by nearly 75%.

The much larger range of muscle stress and higher maximal stresses developed in the kangaroo rat over its full range of locomotor performance compared to that obtained for the pigeon over nearly its full range of flight performance indicates distinctly differing roles for these muscles during hopping and jumping *versus* during flight. In contrast to the pectoralis, which shortens (up to 37% of its resting length) to generate the power required for lift and thrust associated with flight, the ankle extensors of the kangaroo rat (as well as
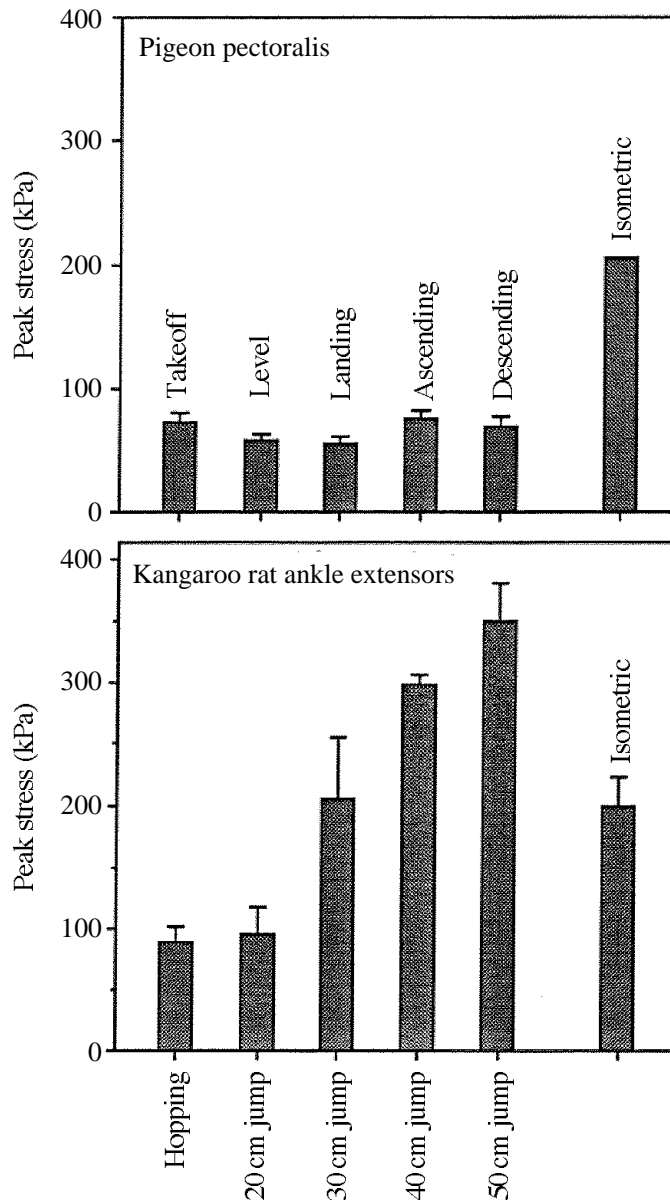
Fig. 14. Histograms showing (A) the range of stress developed in the pigeon pectoralis for the five modes of flight we studied compared to (B) the stresses developed in the ankle extensors of kangaroo rats (*Dipodomys spectabilis*) during hopping and jumping (adapted from Biewener *et al.* 1988). The much larger range of stress and the much higher stresses developed in the kangaroo rat corresponds to its muscles undergoing significant stretch activation during jumping and presumably operating over a much smaller range of muscle strain. Bars show 1 s.e. (hopping $N= 10$; jumping $N= 3–8$; isometric $N= 5$).

other limb muscles of terrestrial mammals generally, Alexander, 1988; Taylor, 1985) act much like 'springs', undergoing significant stretch–shorten contractions during the landing and takeoff phases of the stride. In doing so, these muscles presumably operate over a much smaller range of active muscle length change to generate the extremely high forces that were recorded (Biewener *et al.* 1988). Although our estimate of fiber shortening (37%) within the pigeon pectoralis suggests a decreased ability of the muscle
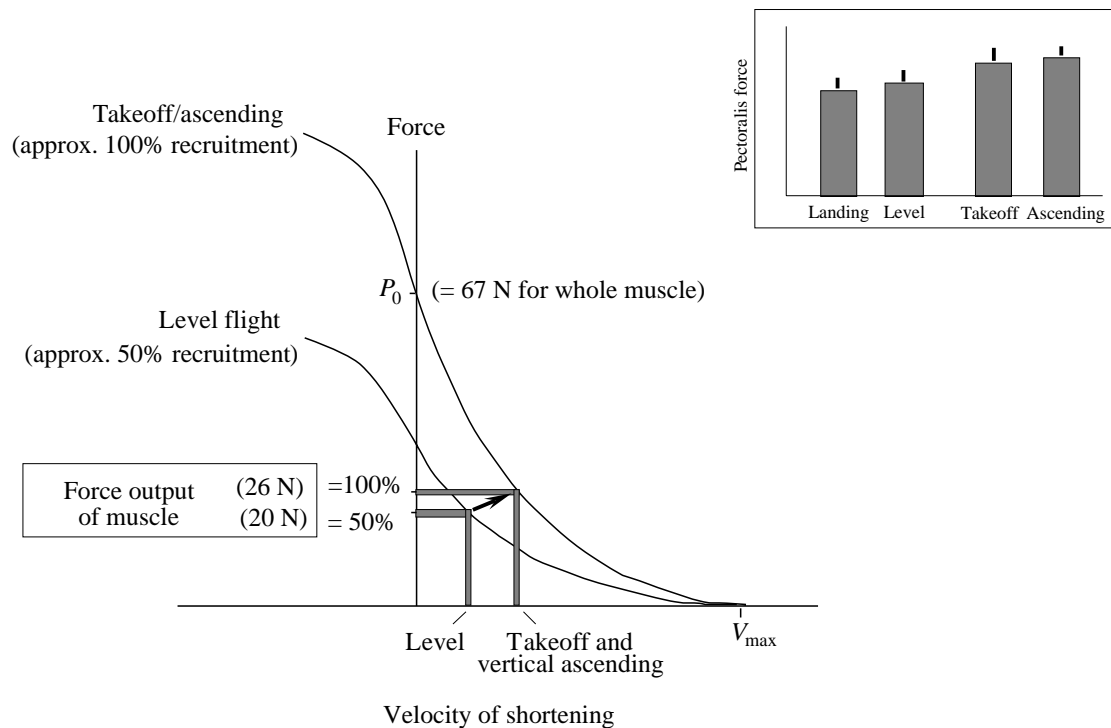
Fig. 15. Hypothetical force–velocity curves for the pigeon during level flight and takeoff or ascending flight. Each curve represents the force output and shortening velocity of the whole muscle. If we assume that 50% of the pectoralis is recruited to generate 20N of force during level flight at the shortening velocity shown (approximately 4.4lengths s^{-1}), then 100% of the pectoralis muscle must be recruited to generate 26N of force at the higher shortening velocity (approximately 6.7length s^{-1}) for takeoff or vertical ascending flight. A twofold increase in power output, therefore, is achieved by a 30% increase in force and a 53% increase in the muscle's shortening velocity (the remaining difference being due to the rate of force development during takeoff and ascending flight; see Fig. 13). The increase in shortening velocity is achieved mainly by an increase in wingbeat amplitude, which nearly doubles (from 80 to 140°) from level flight to takeoff and ascending flight, with wingbeat frequency remaining nearly constant. Inset is adapted from Fig. 12A, showing the relative magnitude of force generated by the pectoralis during each activity.

to generate force late in the downstroke at short muscle lengths, this effect is mitigated by the muscle being stretched by 16% prior to shortening. Consequently, net shortening of the muscle is about 21% of its resting length. Depending on the force–length properties of the muscle, this degree of shortening may not critically impair the muscle's ability to generate force throughout most of the downstroke.

The narrow range of maximal force development (44%, 18–26N) in the pigeon pectoralis associated with generating a 2.3-fold increase in mass-specific mechanical power output (51 *vs* 119 W kg^{-1} muscle), during level flapping flight *versus* takeoff and ascending flight can be understood by considering a simple hypothetical model for the force–velocity relationship of the pectoralis muscle operating under these two conditions (Fig. 15). The lower curve shows the force–velocity curve for the muscle assuming 50 % recruitment of the pectoralis during level flight, operating at a shortening velocity (4.4lengths s^{-1}) that enables it to generate a maximal force of about 20N. The upper

curve depicts the force–velocity curve of the muscle during takeoff/ascending flight, when presumably nearly the entire muscle is activated (100% recruitment). This assumption is partially based on the observation that the integrated area of the rectified EMG of the pectoralis (i.e. EMG intensity) was maximal during takeoff and ascending flight, but 50% of maximum during level flight and descending flight (Fig. 6). During takeoff or vertical ascent, therefore, maximal force generation increases to only 26N (or 39% of isometric) because the muscle contracts at a higher shortening velocity (6.7lengths s^{-1}) to achieve the increase in power needed for these activities. Given that wingbeat frequency varies little among flight modes (8–9Hz), the kinematic variable that changes most significantly to vary muscle shortening velocity and power output is wingbeat amplitude, which nearly doubles from approximately 80° (level flight) to 140° (takeoff and vertical ascending flight). The extremely narrow range of wingbeat frequencies may reflect the fairly homogeneous population of muscle fiber types present within this muscle (based on histological evidence: James and Meek, 1979; Kaplan and Goslow, 1989; Rosser and George, 1986; Talesara and Goldspink, 1978), necessitating that increases in power output are achieved mainly by increases in wingbeat amplitude (muscle shortening distance, Goldspink, 1981). Hence, the pigeon achieves a twofold increase in mechanical power output by roughly equivalent increases in muscle force (44%) and shortening velocity (52%).

Similar to the ankle extensors of running and hopping mammals, the avian pectoralis also undergoes stretch activation. The amount of negative work performed by the pectoralis during lengthening, however, is quite small compared to the positive work generated as it shortens. The short tendinous insertion of the muscle precludes a role in the storage and recovery of elastic strain energy, as is often the case in the muscle–tendon systems of running and hopping mammals (Alexander, 1988). While the negative work performed by the avian pectoralis appears to be associated with the need to counter wing inertia at the end of the upstroke, stretch activation of the muscle also probably enables it to develop force more rapidly, enhancing its ability to perform positive work as it subsequently shortens. Indeed, the need for rapid force development at the onset of contraction and the need to maximize power output when shortening may underlie our observation that the pectoralis does not fully relax by the end of the downstroke (also see Goslow and Dial, 1990).

Although we document here the use of single-element strain gauge recordings of DPC strain as a reliable means for measuring pectoralis force directly during free flight, our estimates of mechanical power output still rely on indirect assessments of muscle length change obtained from high-speed light films taken of the animals during flight. Estimates of average fiber shortening derived from wing kinematics may therefore represent a significant source of error in our calculation of pectoralis work and power output. Moreover, in studies of animals during free flight in still air, such as this, the range of performance for which muscle length changes can be reliably estimated from films is greatly limited. Future studies combining *in vivo* measurements of force development with direct recordings of muscle fiber length change (e.g. Griffiths, 1987) may provide an independent and potentially more reliable measure of the contractile characteristics and power output of this key flight muscle. By obtaining these measurements over a wider

range of flight speeds, we can begin to establish an empirical relationship between power and speed for forward flapping flight.

References

ALEXANDER, R. McN. (1977). Allometry of the limbs of antelopes (Bovidae). *J. Zool., Lond.* **83**, 125–146.

ALEXANDER, R. McN. (1988). *Elastic Mechanisms in Animal Movement*. Cambridge: Cambridge University Press.

BERNSTEIN, M. H., THOMAS, S. P. AND SCHMIDT-NIELSEN, K.(1973). Power input during flight of the fish crow, *Corvusossifragus*. *J. exp. Biol.* **58**, 401–410.

BIEWENER, A. A., BLICKHAN, R., PERRY, A. K., HEGLUND, N. C. AND TAYLOR, C. R. (1988). Muscle forces during locomotion in kangaroo rats: force platform and tendon buckle measurements compared. *J. exp. Biol.* **137**, 191–205.

BIEWENER, A. A., DIAL, K. P. AND GOSLOW, G. E., JR (1992). Pectoralis muscle force and power output during flight in the starling. *J. exp. Biol.* **164**, 1–18.

BROWN, R. J. H. (1948). The flight of birds. I. The flapping cycle of the pigeon. *J. exp. Biol.* **7**, 322–333.

BROWN, R. J. H. (1963). The flight of birds. *Biol. Rev.* **38**, 460–489.

CONLEY, K. E., KAYAR, S. R., ROSLER, K., HOPPELER, H., WEIBE, L. E. R. AND TAYLOR, C. R. (1987). Adaptive variation in the mammalian respiratory system in relation to energetic demand. IV. Capillaries and their relationship to oxidative capacity. *Respir. Physiol.* **69**, 47–64.

DALLY, J. F. AND REILLY, W. F.(1978). *Experimental Stress Analysis.* New York: McGraw-Hill.

DIAL, K. P.(1992). Activity patterns of the wing muscles of the pigeon (*Columbalivia*) during different modes of flight.*J. exp. Zool.* **262**, 357–373.

DIAL, K. P., KAPLAN, S. R. AND GOSLOW, G. E., JR (1988). A functional analysis of the primary upstroke and downstroke muscle in the domestic pigeon (*Columba livia*) during flight. *J.exp. Biol.* **134**, 1–16.

ELLINGTON, C. P. (1991). Limitations on animal flight performance. *J. exp. Biol.* **160**, 71–91.

ELLINGTON, C. P., MACHIN, K. E. AND CASEY, T. M. (1990). Oxygen consumption of bumblebees in forward flight. *Nature* **347**, 472–473.

GAUNT, A. S. AND GANS, C. (1990). Architecture of chicken muscles: short fiber patterns and their ontogeny. *Trans. R. Soc. Lond. B* **240**, 351–362.

GOLDSPINK, G. (1981). The use of muscles during flying, swimming and running from the point of view of energy saving. *Symp. zool. Soc., Lond.* **48**, 219–238.

GOSLOW, G. E. AND DIAL, K. P. (1990). Active stretch-shorten contractions of the m. pectoralis in the European starling (*Sturnus vulgaris*): evidence from electromyography and contractile properties. *Netherlands J. Zool.* **40**, 106–114.

GREENEWALT, C. H.(1975). The flight of birds. *Trans. Am. Phil. Soc.* **65**, 1–67.

GRIFFITHS, R. I. (1987). Ultrasound transit time gives direct measurement of muscle fiber length *in vivo*. *J. Neurosc. Meth.* **21**, 159–165.

HEGLUND, N. C., FEDAK, M. A., TAYLOR, C. R. AND CAVAGNA, G. A. (1982). Energetics and mechanics of terrestrial locomotion. IV. Total mechanical energy changes as a function of speed and body size in birds and mammals.*J. exp. Biol.* **97**, 57–66.

JAMES, N. T. AND MEEK, G. A. (1979). Stereological analyses of the structure of mitochondria in pigeon skeletal muscle. *Cell Tissue Res.* **202**, 493–503.

JOSEPHSON, R. K. (1985). Mechanical power output from striated muscle during cyclic contraction. *J. exp. Biol.* **114**, 493–512.

KAPLAN, S. R. AND GOSLOW, G. E., JR (1989). Neuromuscular organization of the pectoralis (pars thoracicus) of the pigeon (*Columbalivia*): Implications for motor control. *Anat. Rec.* **224**, 426–430.

LAKES, R. S., KATZ, J. L. AND STERNSTEIN, S. S. (1979). Viscoelastic properties of wet cortical bone. I. Torsional and biaxial studies. *J. Biomech.* **12**, 657–678.

LIGHTHILL, J. (1977). Introduction to the scaling of aerial locomotion. In *Scale Effects in Animal Locomotion* (ed. T. J. Pedley), pp. 365–404. London: Academic Press.

LOEB, G. E. AND GANS, C. (1986). *Electromyography for Experimentalists*. Chicago: University of Chicago Press.

MARDEN, J. H. (1987). Maximum lift production during takeoff in flying animals. *J. exp. Biol.* **130**, 527–555.

PENNYCUICK, C. J.(1968). Power requirements for horizontal flight in the pigeon (*Columbalivia*). *J. exp. Biol.* **49**, 527–555.

PENNYCUICK, C. J.(1975). Mechanics of flight. In *Avian Biology*, vol. V. London: Academic Press

PENNYCUICK, C. J. (1989). *Bird Flight Performance. A Practical Calculation Manual*. Oxford: Oxford University Press.

ROSSER, B. W. C. AND GEORGE, J. C. (1986). The avian pectoralis: histochemical characterization and distribution of muscle fiber types. *Can. J. Zool.* **64**, 1174–1185.

ROTHE, H.-J. AND NACHTIGALL, W. (1987). Pigeon flight in a wind tunnel. *J. comp. Physiol.* B **157**, 91–98.

STEVENSON, R. D. AND JOSEPHSON, R. K. (1990). Effects of operating frequency and temperature on mechanical power output from moth flight muscle. *J. exp. Biol.* **149**, 61–78.

TALESARA, G. L. AND GOLDSPINK, G. (1978). A combined histochemical or biochemical study of myofibrillar ATPase in pectoral, leg and cardiac muscle of several species of bird. *Histochem. J.* **10**, 695–710.

TAYLOR, C. R.(1985). Force development during sustained locomotion: a determinant of gait, speed and metabolic power. *J. exp. Biol.* **115**, 253–262.

THOMAS, S. P. (1975). Metabolism during flight in two species of bats, *Phyllostomus hastatus* and *Pteropusgouldii*. *J. exp. Biol.* **63**, 273–293.

TORRE-BUENO, J. R. AND LAROCHELLE, J.(1978). The metabolic cost of flight in unrestrained bird. *J.exp. Biol.* **75**, 223–229.

TROTTER, J. A., SALGADO, J. D., OZBAYSAL, R. AND GAUNT, A. S. (1992). The composite structure of quail pectoralis muscle. *J. Morph.* **212**, 27–35.

TUCKER, V. A.(1968). Respiratory exchange and evaporative water loss in the flying budgerigar. *J. exp. Biol.* **48**, 67–87.

TUCKER, V. A. (1972). Metabolism during flight in the laughing gull, *Larus atricilla*. *Am. J. Physiol.* **222**, 237–245.

WEIS-FOGH, T. AND ALEXANDER, R. MCN. (1977). The sustained power output from striated muscle. In *Scale Effects in Animal Locomotion* (ed. T. J. Pedley), pp. 511–525. London: Academic Press.